Supplement of Earth Surf. Dynam., 11, 461–474, 2023
https://doi.org/10.5194/esurf-11-461-2023-supplement
© Author(s) 2023. CC BY 4.0 License.

Earth Surface Dynamics
Open Access
EGU

Supplement of

Revealing the relation between spatial patterns of rainfall return levels and landslide density

Slim Mtibaa and Haruka Tsunetaka

Correspondence to: Slim Mtibaa (mtibaaslim@ffpri.affrc.go.jp)

The copyright of individual parts of the supplement might differ from the article licence.

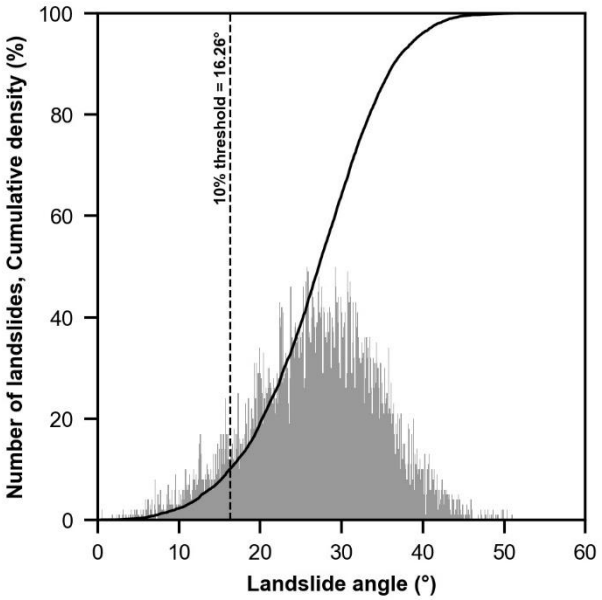

Figure S1: Non-cumulative (gray histogram) and cumulative (black line) frequency distribution of landslide angle

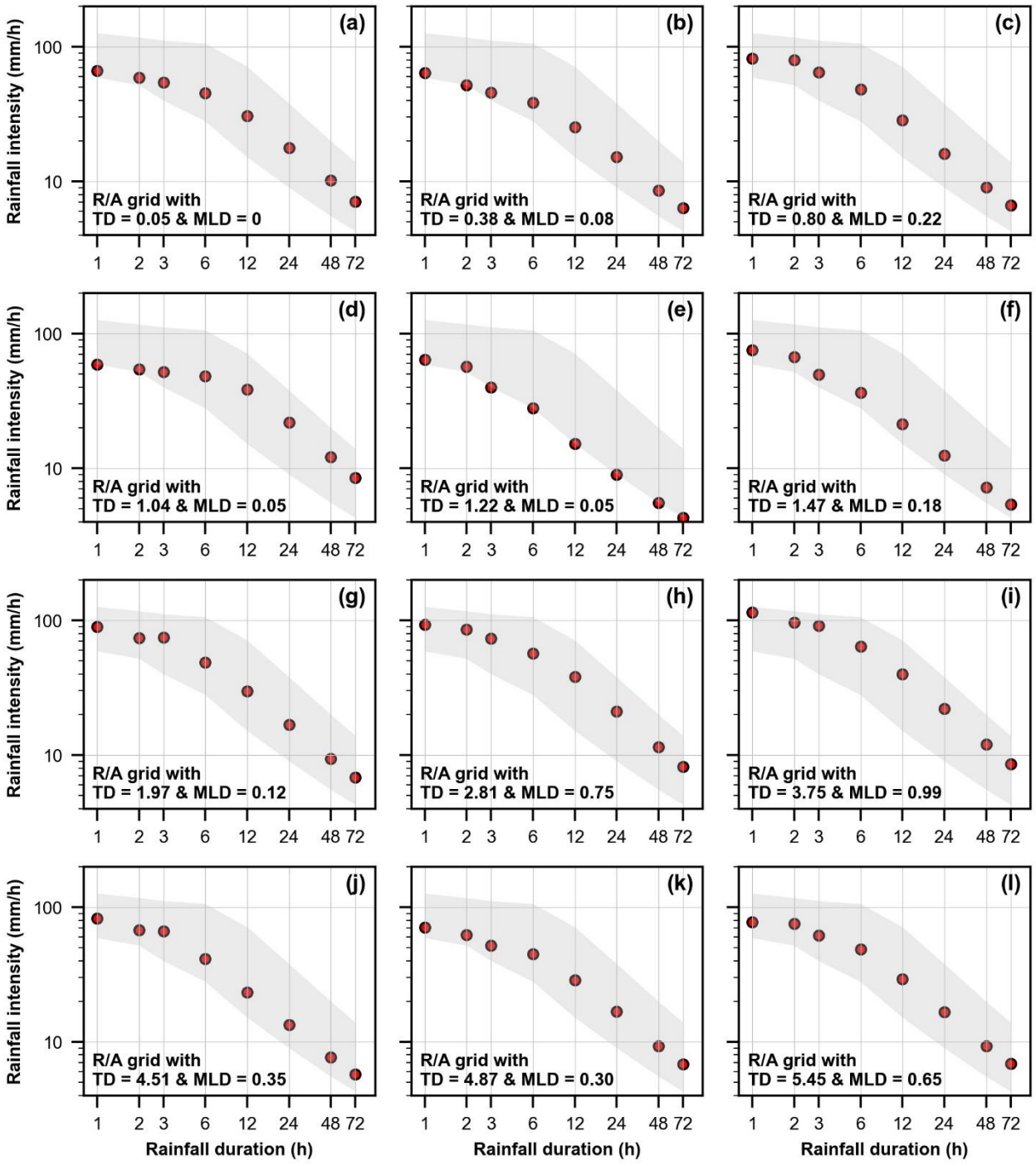
(a)
R/A grid with
TD = 0.05 & MLD = 0
(b)
R/A grid with
TD = 0.38 & MLD = 0.08
(c)
R/A grid with
TD = 0.80 & MLD = 0.22
(d)
R/A grid with
TD = 1.04 & MLD = 0.05
(e)
R/A grid with
TD = 1.22 & MLD = 0.05
(f)
R/A grid with
TD = 1.47 & MLD = 0.18
(g)
R/A grid with
TD = 1.97 & MLD = 0.12
(h)
R/A grid with
TD = 2.81 & MLD = 0.75
(i)
R/A grid with
TD = 3.75 & MLD = 0.99
(j)
R/A grid with
TD = 4.51 & MLD = 0.35
(k)
R/A grid with
TD = 4.87 & MLD = 0.30
(l)
R/A grid with
TD = 5.45 & MLD = 0.65
Rainfall intensity (mm/h)
100
10
1 2 3 6 12 24 48 72
Rainfall duration (h)

5

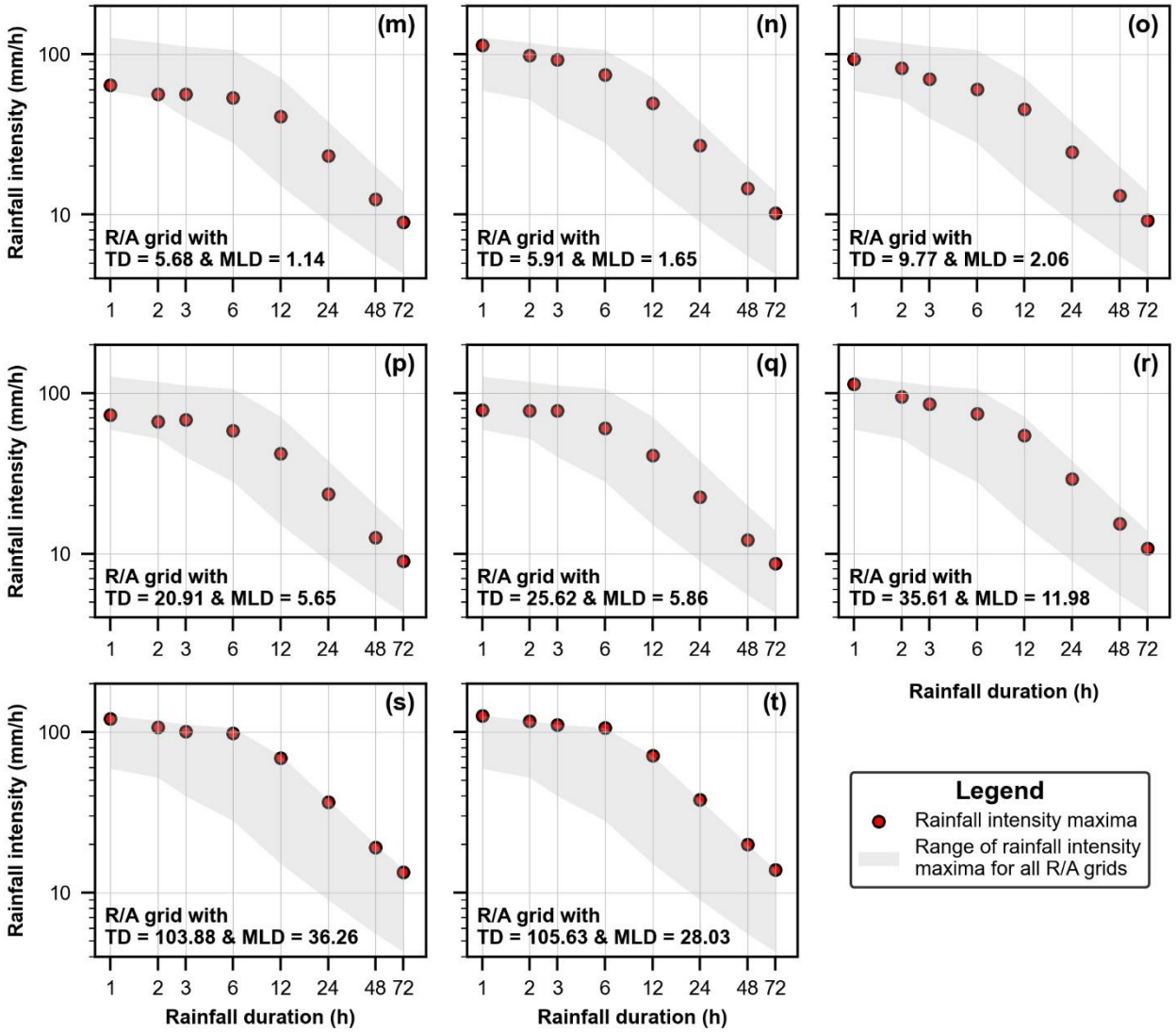

Figure S2: Rainfall intensity maxima for multiple timespans (1–72 h) within the P_{std} for the different R/A grid cells (excluding three R/A grid cells where landslide occurrence was deemed to be affected by anthropogenic activities).

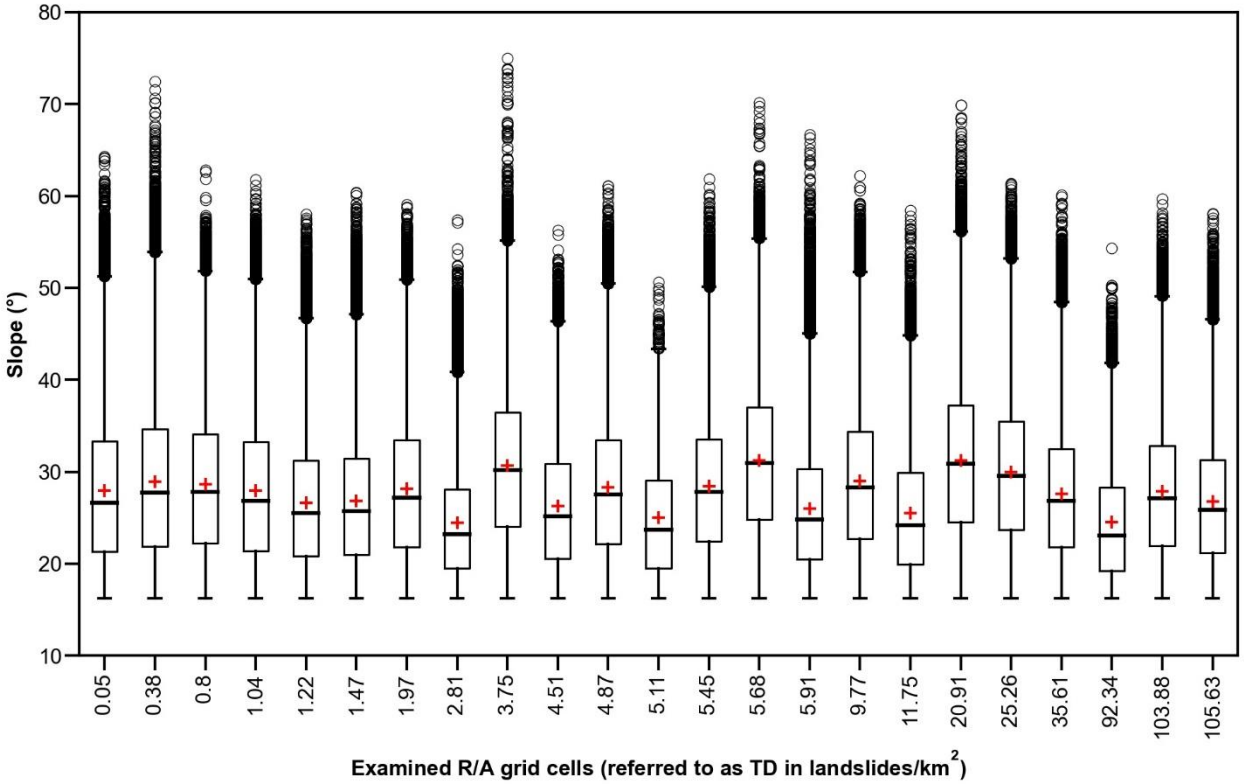

Figure S3: Distribution of local slopes within $A_{threshold}$ of the R/A grid cells. Note that the distributions are shown as box-and-whisker plots. The box delimitates the 25th and 75th percentiles. The black line indicates the median. The red cross '+' displays the mean. The circles 'o' designate the outliers.

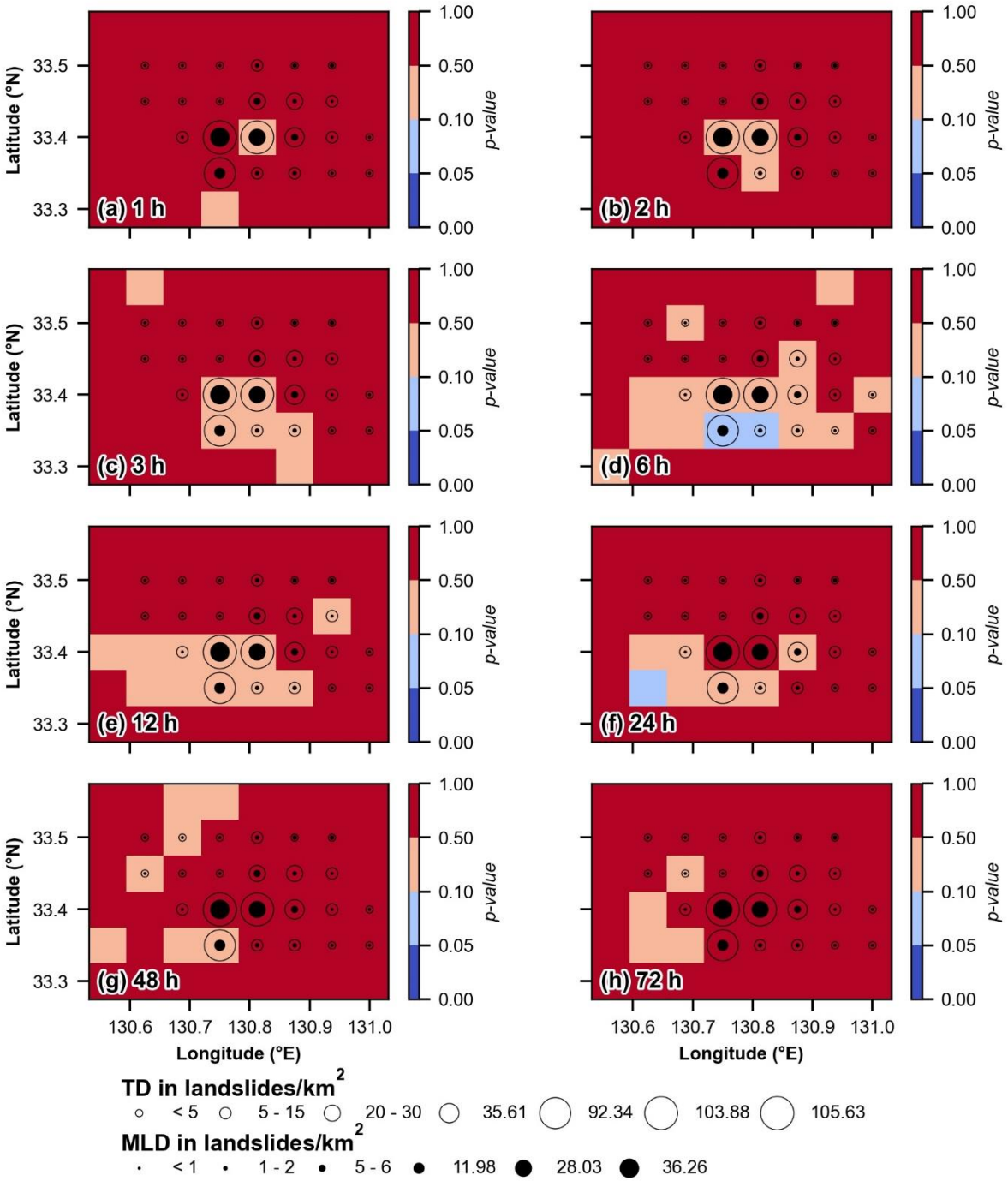

15

Figure S4: Spatial distribution maps of *p-values* resulted from the Kolmogorov-Smirnov test

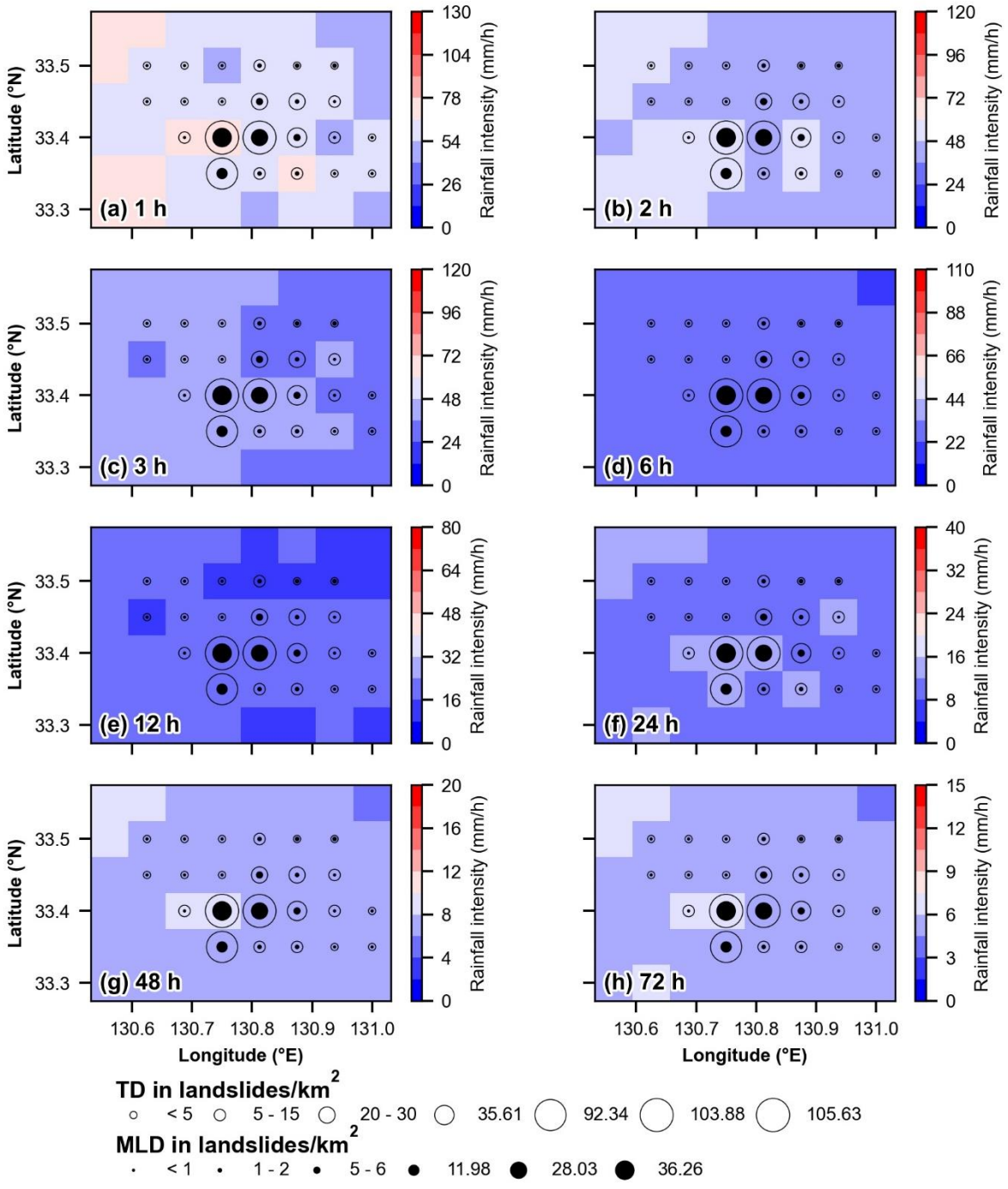

Figure S5: Estimated rainfall intensities for 5-year return period

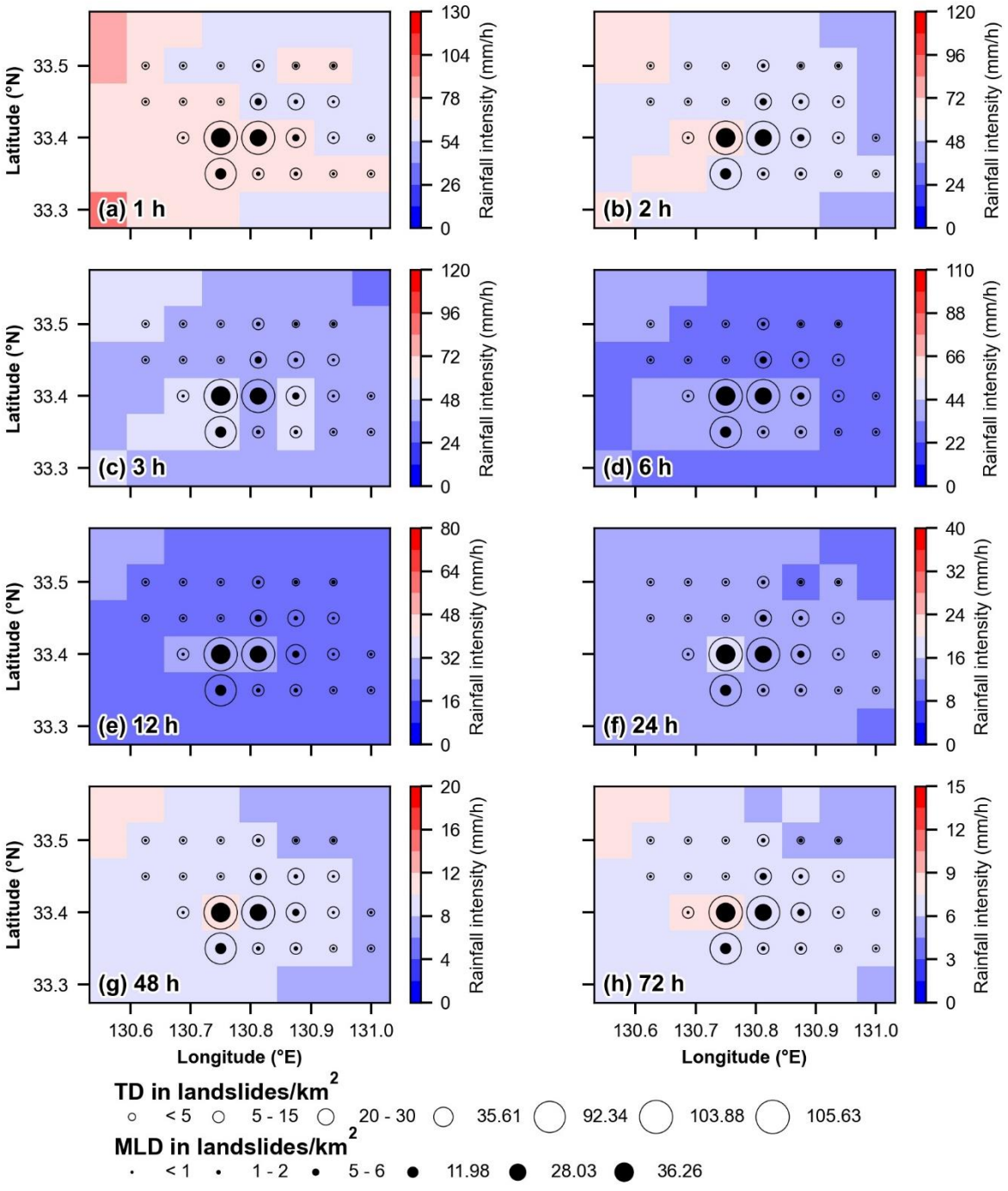

Figure S6: Estimated rainfall intensities for 10-year return period

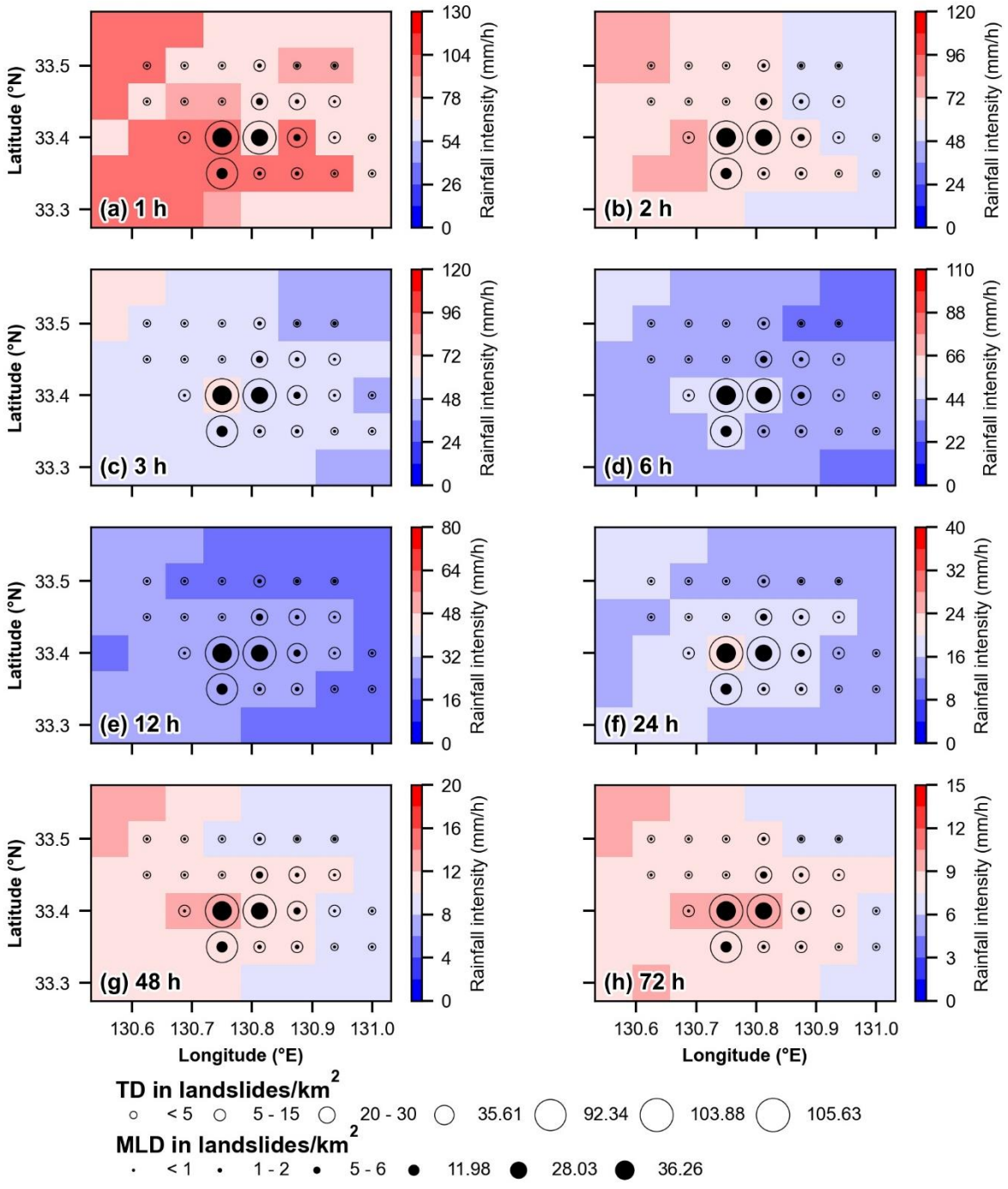

Figure S7: Estimated rainfall intensities for 25-year return period

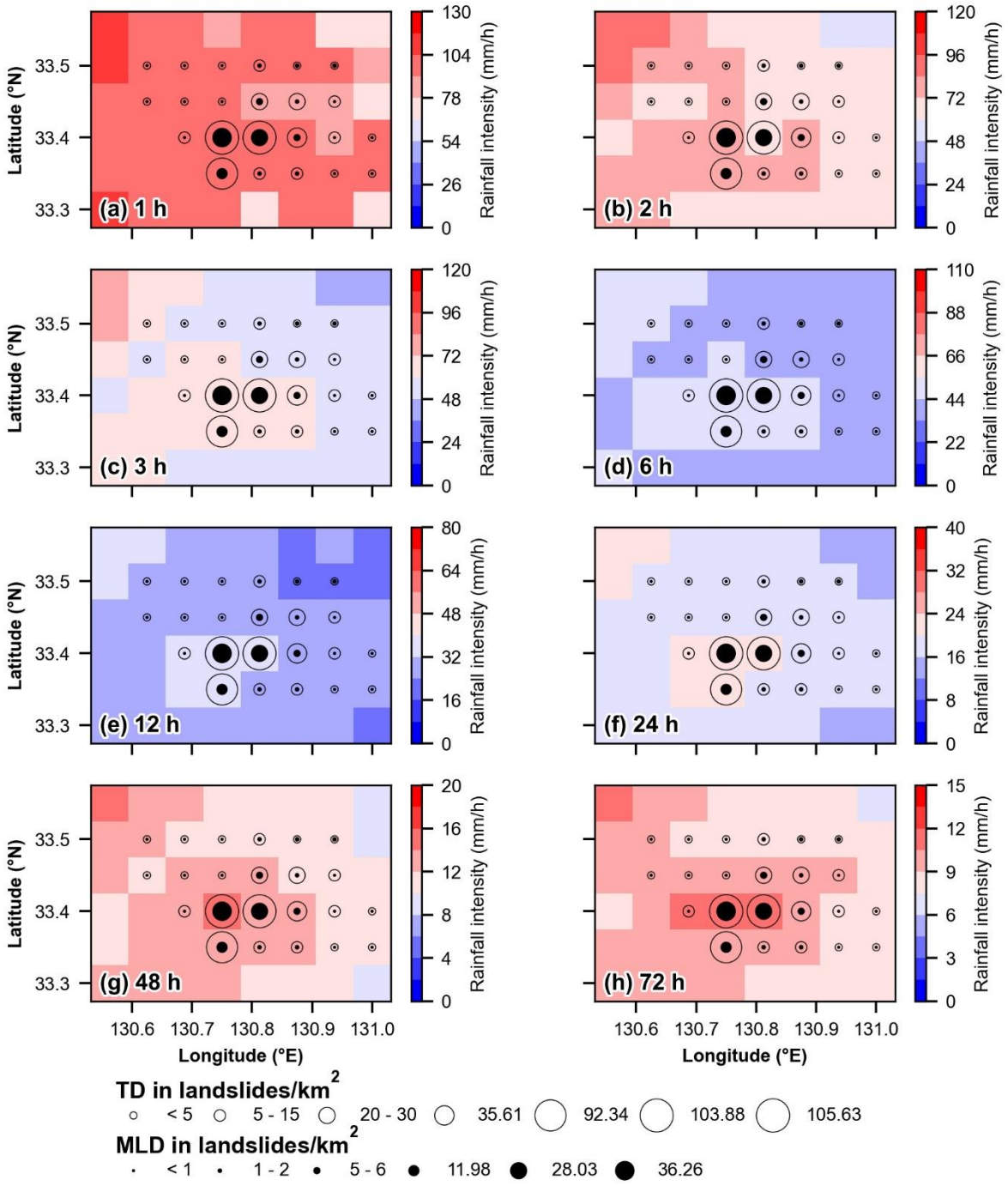

Figure S8: Estimated rainfall intensities for 50-year return period

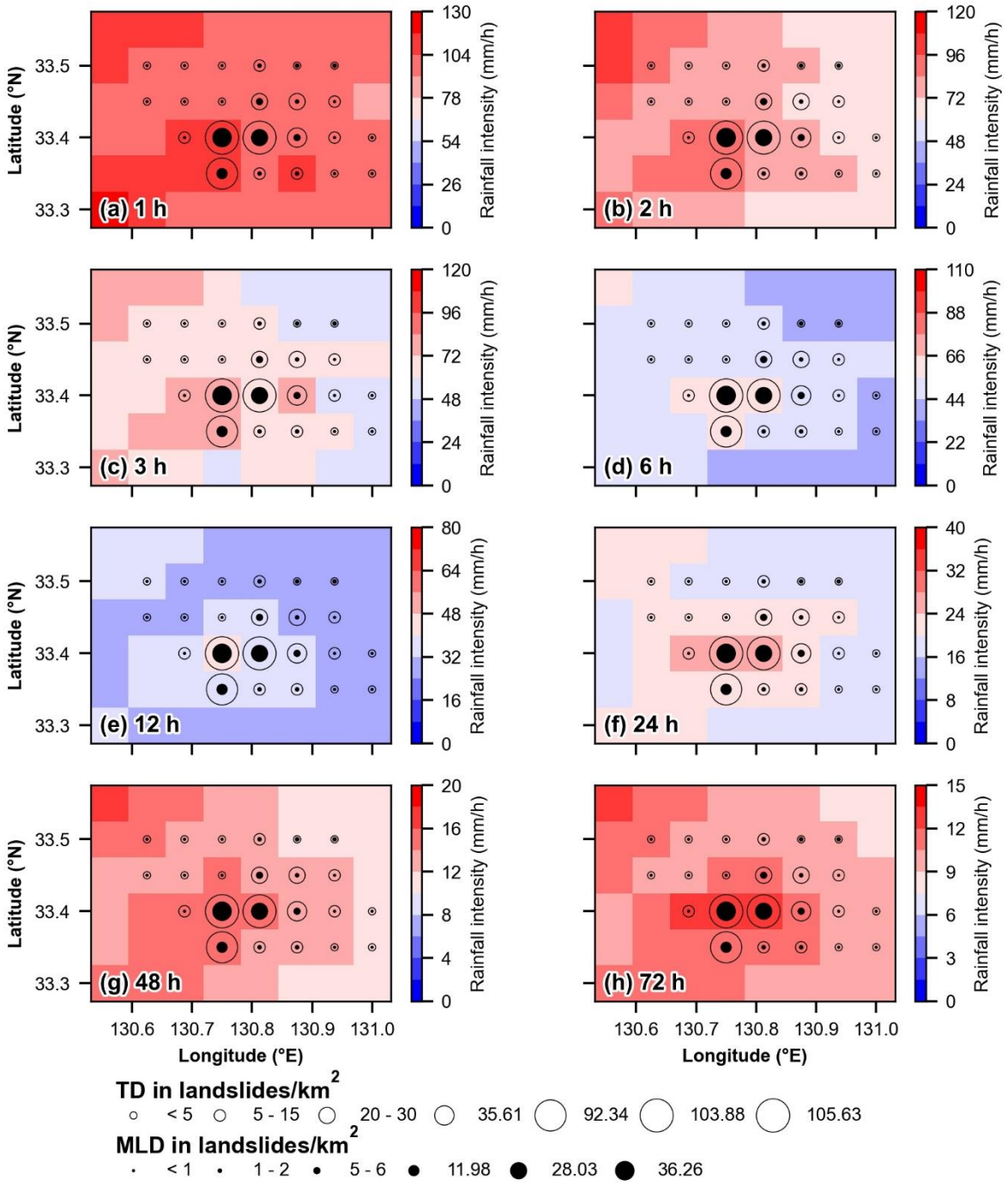

Figure S9: Estimated rainfall intensities for 100-year return period

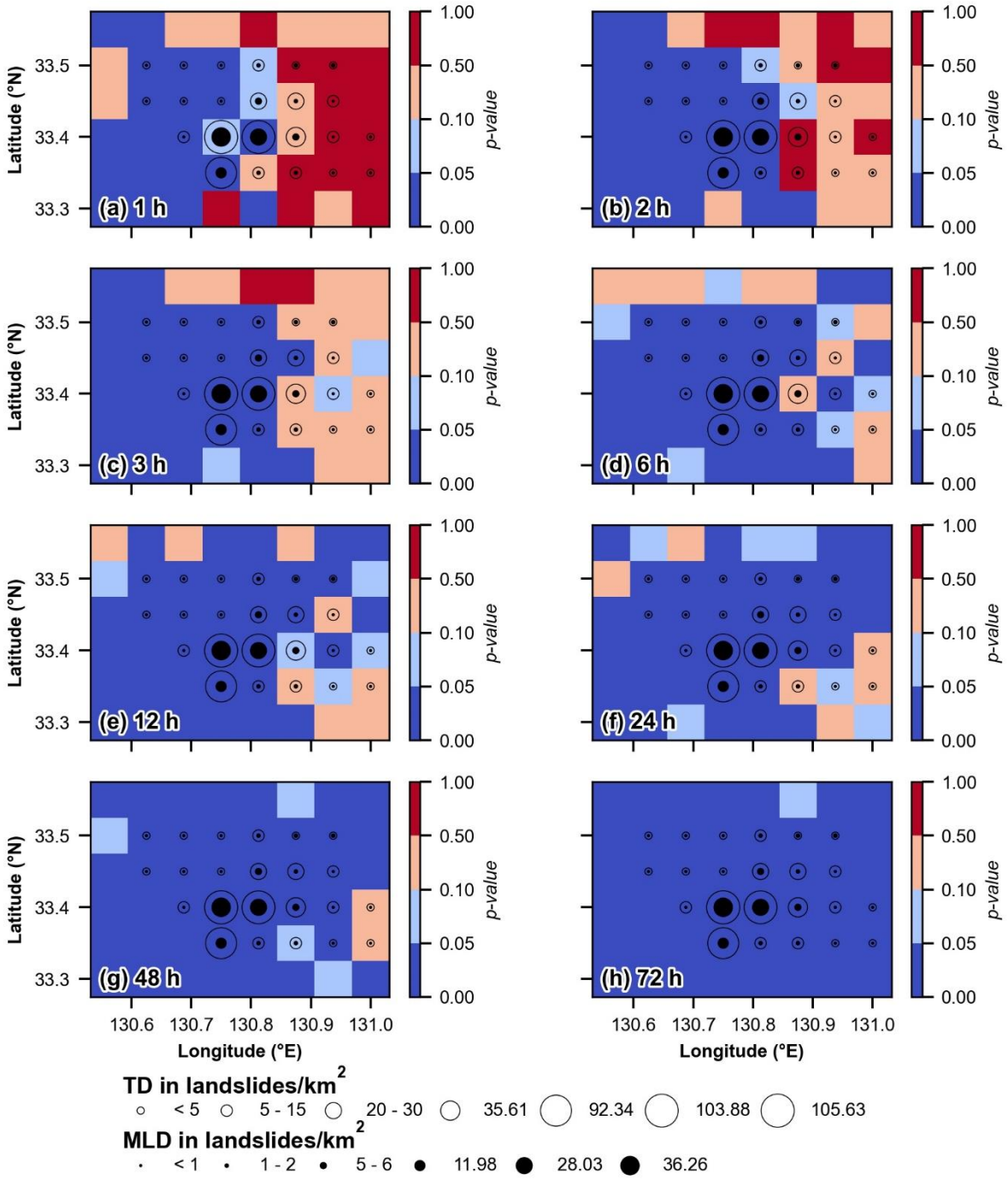

6

Figure S10: Spatial distribution maps of *p-values* resulted from the Mann-Kendall test

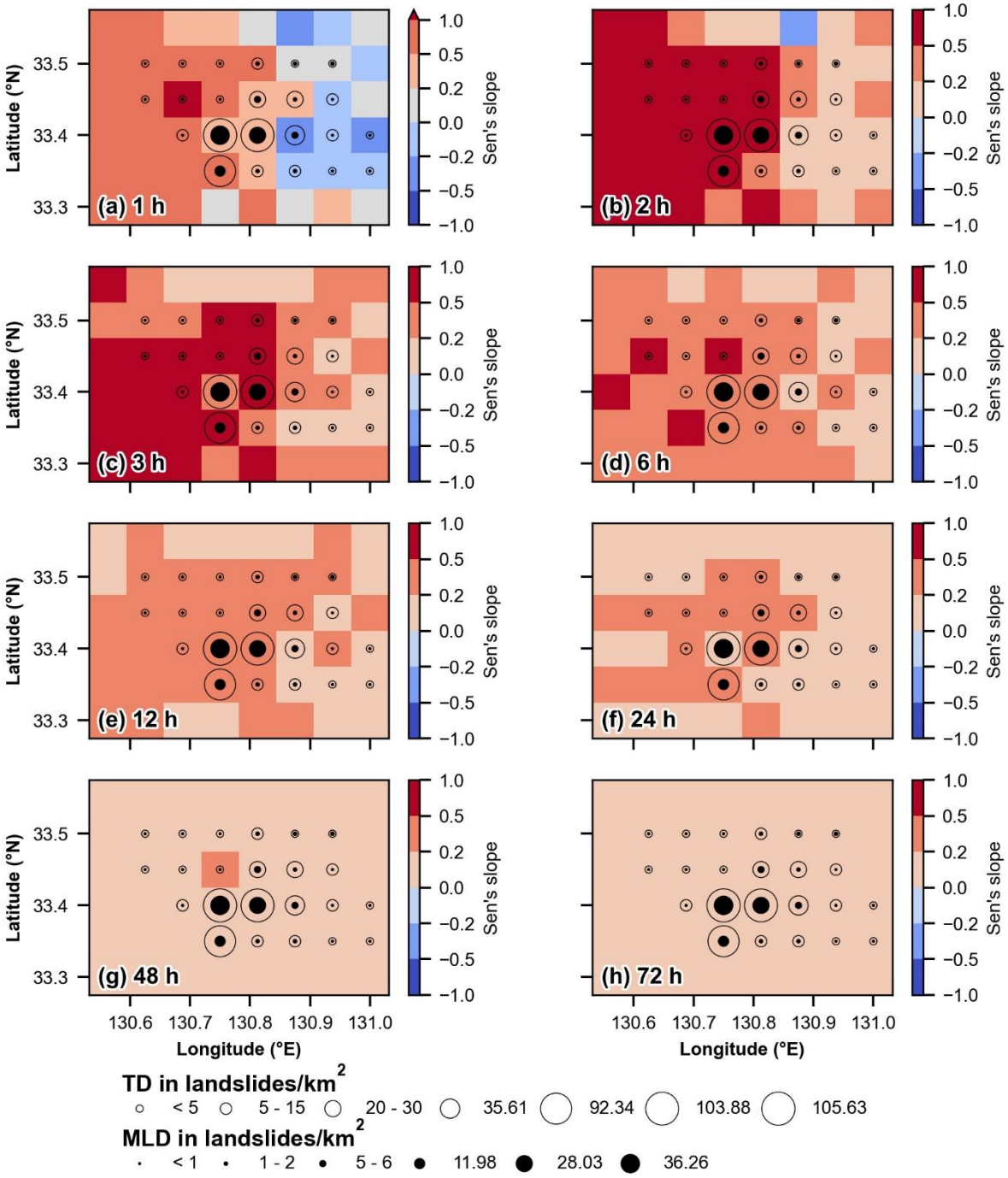

Figure S11: Spatial distribution maps of Sen's slope

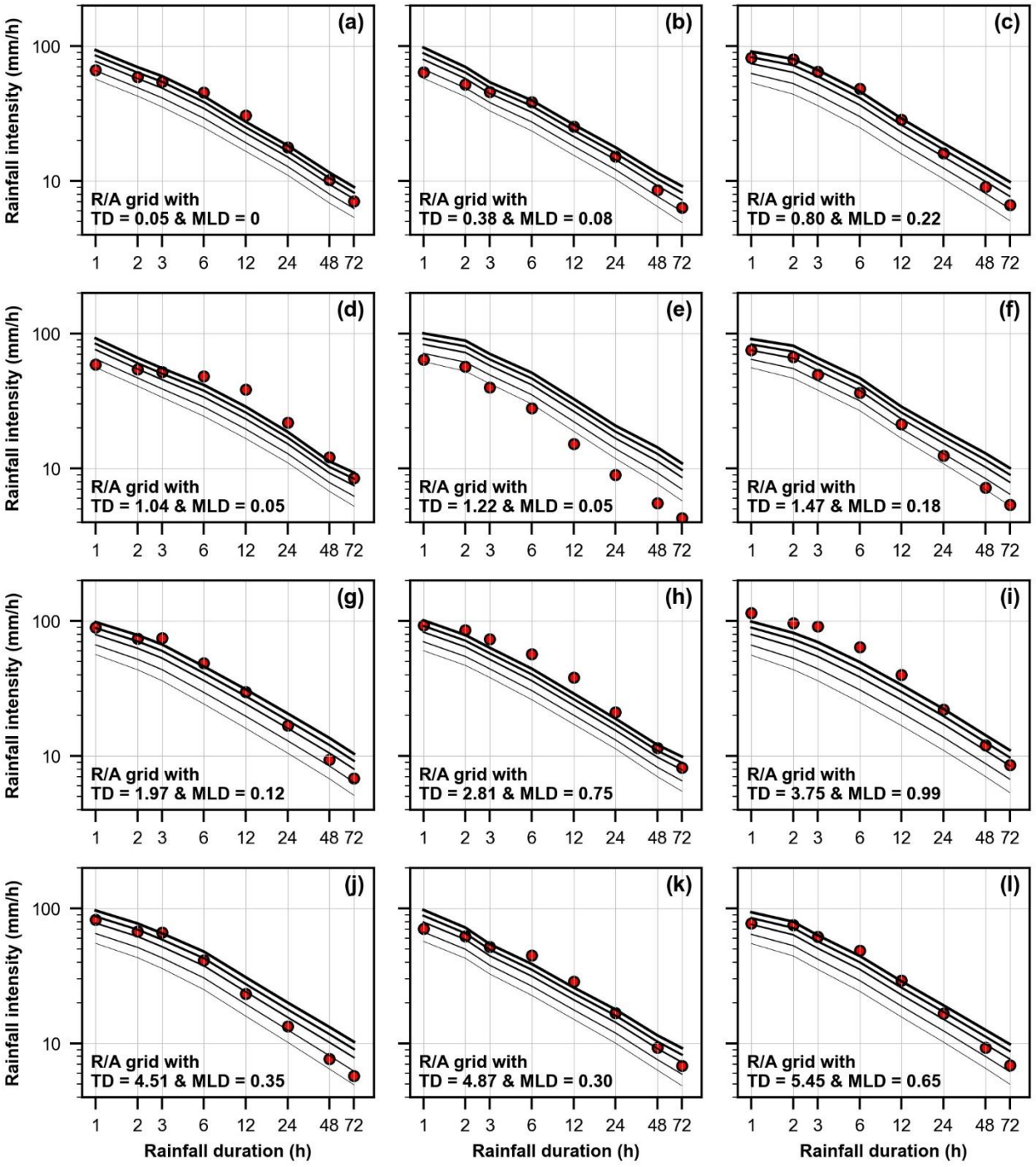
(a)
R/A grid with
TD = 0.05 & MLD = 0
(b)
R/A grid with
TD = 0.38 & MLD = 0.08
(c)
R/A grid with
TD = 0.80 & MLD = 0.22
(d)
R/A grid with
TD = 1.04 & MLD = 0.05
(e)
R/A grid with
TD = 1.22 & MLD = 0.05
(f)
R/A grid with
TD = 1.47 & MLD = 0.18
(g)
R/A grid with
TD = 1.97 & MLD = 0.12
(h)
R/A grid with
TD = 2.81 & MLD = 0.75
(i)
R/A grid with
TD = 3.75 & MLD = 0.99
(j)
R/A grid with
TD = 4.51 & MLD = 0.35
(k)
R/A grid with
TD = 4.87 & MLD = 0.30
(l)
R/A grid with
TD = 5.45 & MLD = 0.65
Rainfall intensity (mm/h)
100
10
1 2 3 6 12 24 48 72
Rainfall duration (h)

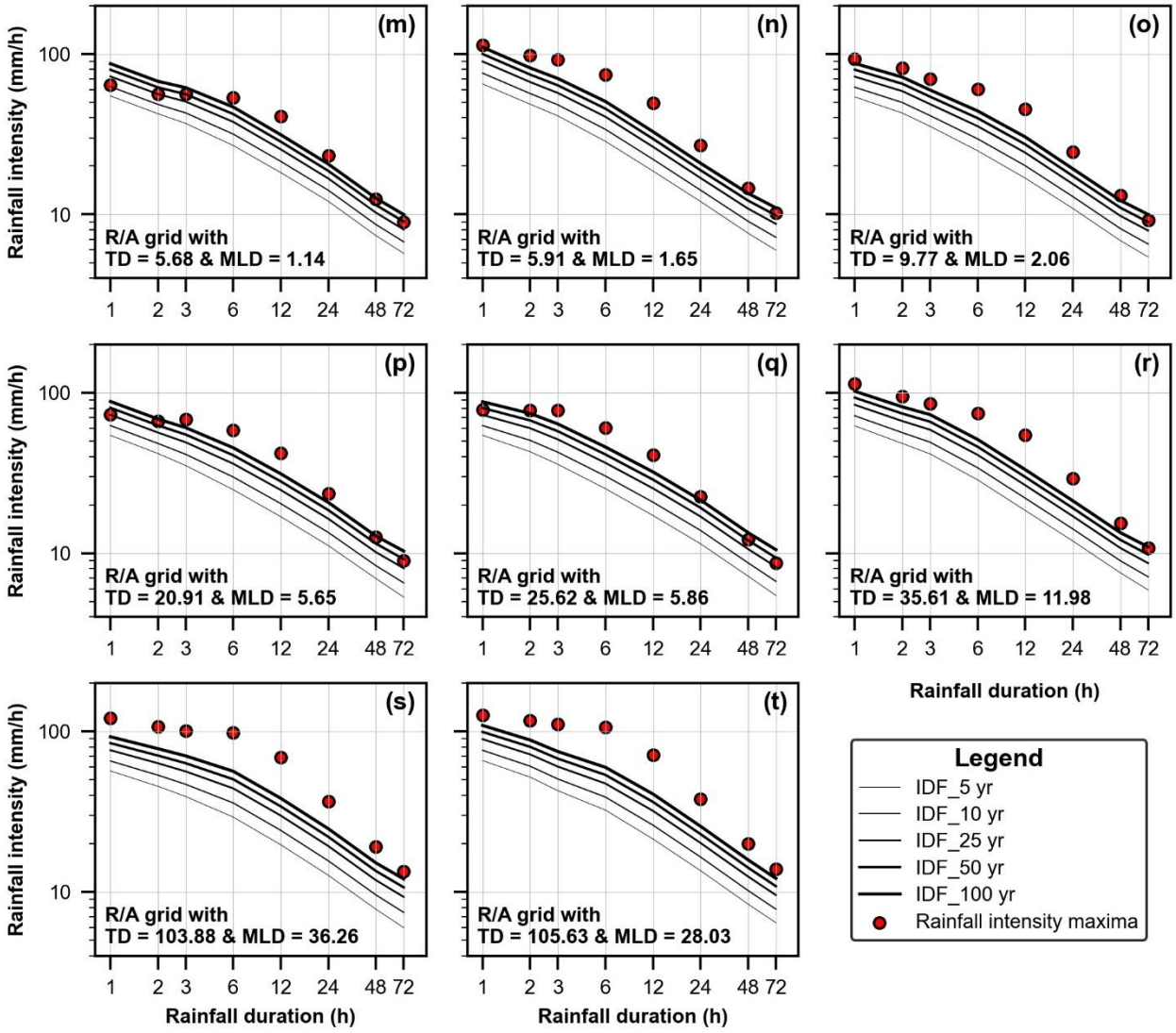

Figure S12: IDF curves and rainfall intensity maxima for multiple timespans (1 – 72 h) within the P_{std} for the different R/A grid cells (excluding three R/A grid cells where landslide occurrence was deemed to be affected by anthropogenic activities).

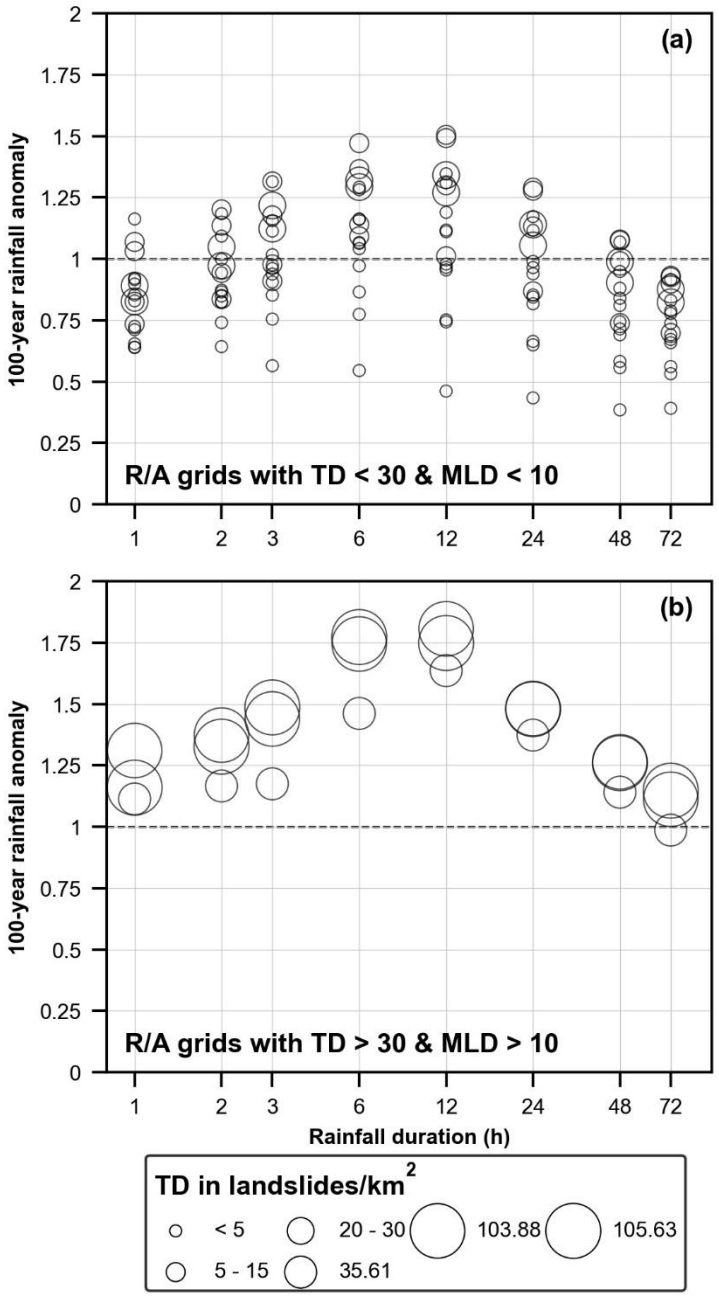

Figure S13: Variation of the 100-year rainfall anomaly at multiple timespans over the R/A grid cells with low (a) and high landslide density (b) (excluding three R/A grid cells where landslide occurrence was deemed to be affected by anthropogenic activities).

Table S1. Adjusted *p-values* from multiple pairwise comparisons of slope distributions within $A_{threshold}$ using the Dunn's test. The analysis expected three R/A grid cells, where most landslides occurred in areas affected by anthropogenic activities (e.g., slopes surrounding cropland and paddy field). The null hypothesis assumes no significant differences in slope distributions. A *p-value* higher than a significant level of 5 % leads to accept the null hypothesis. The test was applied after rejecting the null hypothesis of the Kruskal-Wallis static, which indicated significant differences in slope distributions within $A_{threshold}$ of the R/A grid cells.

TD	0.05	0.38	0.8	1.04	1.22	4.51	2.81	1.47	1.97	3.75	4.87	5.91	5.45	5.68	9.77	20.91	25.26	35.61	105.63	103.88
0.05	1.00																			
0.38	0.00	1.00																		
0.8	0.00	1.00	1.00																	
1.04	1.00	0.00	0.00	1.00																
1.22	0.00	0.00	0.00	0.00	1.00															
4.51	0.00	0.00	0.00	0.00	0.00	1.00														
2.81	0.00	0.00	0.00	0.00	0.00	0.00	1.00													
1.47	0.00	0.00	0.00	0.00	0.00	0.00	0.00	1.00												
1.97	0.00	0.00	0.00	0.00	0.00	0.00	0.00	0.00	1.00											
3.75	0.00	0.00	0.00	0.00	0.00	0.00	0.00	0.00	0.00	1.00										
4.87	0.00	0.00	0.00	0.00	0.00	0.00	0.00	0.00	0.00	0.00	1.00									
5.91	0.00	0.00	0.00	0.00	0.00	0.00	0.00	0.00	0.00	0.00	0.00	1.00								
5.45	0.00	0.01	0.08	0.00	0.00	0.00	0.00	0.00	0.00	0.00	0.00	0.00	1.00							
5.68	0.00	0.00	0.00	0.00	0.00	0.00	0.00	0.00	0.00	0.00	0.00	0.00	0.00	1.00						
9.77	0.00	0.00	0.00	0.00	0.00	0.00	0.00	0.00	0.00	0.00	0.00	0.00	0.00	0.00	1.00					
20.91	0.00	0.00	0.00	0.00	0.00	0.00	0.00	0.00	0.00	0.00	0.00	0.00	0.00	1.00	0.00	1.00				
25.26	0.00	0.00	0.00	0.00	0.00	0.00	0.00	0.00	0.00	0.00	0.00	0.00	0.00	0.00	0.00	0.00	1.00			
35.61	1.00	0.00	0.00	0.01	0.00	0.00	0.00	0.00	0.00	0.00	0.00	0.00	0.00	0.00	0.00	0.00	0.00	1.00		
105.63	0.00	0.00	0.00	0.00	0.00	0.00	0.00	1.00	0.00	0.00	0.00	0.00	0.00	0.00	0.00	0.00	0.00	0.00	1.00	
103.88	0.00	0.00	0.00	0.01	0.00	0.00	0.00	0.00	0.00	0.00	0.00	0.00	0.00	0.00	0.00	0.00	0.00	0.00	0.00	1.00

Table S2: Spearman rank correlations between rainfall intensity maxima

Duration (h)	1	2	3	6	12	24	48	72
1	1							
2	0.97	1						
3	0.93	0.93	1					
6	0.83	0.86	0.94	1				
12	0.71	0.74	0.85	0.96	1			
24	0.71	0.73	0.85	0.96	1	1		
48	0.70	0.72	0.84	0.95	1	1	1	
72	0.71	0.74	0.84	0.96	1	1	1	1